Structure and Thermal/Mechanical Properties of Poly(ϵ-caprolactone)–Clay Blend

GUILLERMO JIMENEZ, NOBUO OGATA, HIDEKAZU KAWAI, TAKASHI OGIHARA

Department of Materials Science and Engineering, Fukui University, Bunkyo 3-9-1, Fukui 910, Japan

Received 16 July 1996; accepted 7 November 1996

ABSTRACT: Montmorillonite was organically modified with distearyldimethylammonium chloride. This organically modified clay (OMON) and poly(ϵ-caprolactone) (PCL) were solvent-cast blended with chloroform, and the structure and properties of the resulting PCL–clay blends were investigated. From isothermal crystallization experiments, it was found that a small amount of OMON in the blend accelerated the crystallization of PCL, whereas a large amount of the organophilic clay delayed it. From small- and wide-angle X-ray scattering measurements, it was found that the silicate layers forming the clay could not be dispersed individually in the PCL blends. In other words, the clay seemed to exist as the tactoids consisting of some silicate layers. These tactoids formed a remarkable geometric structure; that is, their surface planes lay almost parallel to the blend film surface. Furthermore, the tactoids were stacked with insertion of PCL lamellae in the film-thickness direction. Preferred orientation of the PCL crystallites was induced by the presence of the clay. During the drawing process of the blends, fibrillation took place with formation of planelike voids developed on the plane parallel to the film surface. From dynamic viscoelastic measurements, it was shown that intercalation of PCL chains into the layered silicates did not take place in the blends prepared by the solvent-cast method used in this work. © 1997 John Wiley & Sons, Inc. J Appl Polym Sci **64:** 2211–2220, 1997

Key words: montmorillonite; poly(ϵ-caprolactone); nanocomposites; superstructure; intercalation

INTRODUCTION

Inorganic particles are widely used as reinforcement materials for polymers. Among these inorganic materials, clay has been receiving special attention in the field of nanocomposites because of its small particle size and its intercalation properties.[1] Besides economic and environmental factors, its natural abundance, high mechanical strength, and chemical resistance, make clay a useful filler in polymer composites.

Polymers have been intercalated into the layered silicates of clay mainly by two approaches: insertion of a suitable monomer and subsequent polymerization, and direct insertion of polymer chains from solution or the melt. By using the first method, nylon 6–clay hybrids (NCH) have been developed.[2] It was reported that silicate layers in NCH were individually well dispersed in the nylon-6 matrix, and that these hybrids showed good physical properties, e.g., high modulus, high distortion temperature,[3] and good water-barrier property.[4]

Our main research has focused on the synthesis of polymer–clay composites by using polymer intercalation from solution into a layered smectite-type clay known as montmorillonite (MON). Owing to its hydrophilic nature, MON cannot be homogeneously dispersed into the organic polymer phase. Therefore, organically modified montmo-

Correspondence to: N. Ogata.

 CCC 0021-8995/97/112211-10

rillonite (OMON) has been obtained by a cation-exchange reaction.

Besides nylon 6, other polymers such as polyimide,[5] epoxy resin,[6] and poly(ϵ-caprolactone) (PCL)[7] have been focused as matrices for polymer–clay composites. We have also investigated the structure and properties of poly(L-lactide) (PLLA)–clay blends, which were prepared by using chloroform as cosolvent.[8] Although the silicate layers were not individually well dispersed in the PLLA–clay blends, they formed a notable geometric arrangement, namely, the tactoids. In addition, these tactoids, consisting of several silicate layers, were found to be stacked with insertion of PLLA crystalline lamellae, and showed a long period in the thickness direction of the blends. Our interest in the present study is to investigate whether such geometry is commonly observed in solvent-cast blends.

PCL is a biodegradable aliphatic polyester that is currently studied for degradable packaging purposes. It has low-temperature adhesiveness, the ability to disperse pigments, and miscibility with various available polymers such as poly(vinyl chloride) and acrylonitrile–butadiene–styrene copolymer, among others.[9] However, PCL shows a low glass transition (T_g) and a low melting temperature (T_m) (about −55 and 65°C, respectively), which limit further potential applications of the polymer. Then, if the mechanical properties of PCL were improved by the addition of a small quantity of an environmentally benign material such as clay, this polymer would have structural material applications in many fields. PCL–silicate nanocomposites have recently been synthesized by mixing the organically modified mica-type silicate with ϵ-caprolactone, followed by the monomer polymerization. It was reported that this composite exhibited a significant reduction in water-vapor permeability.[10]

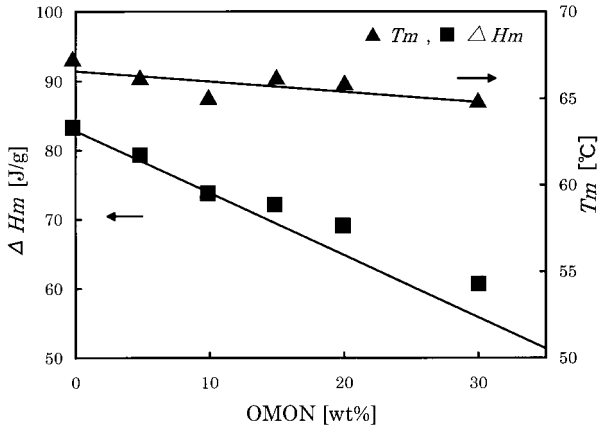

Figure 1 Effect of clay content on PCL melting temperature, T_m, and heat of fusion, ΔH_m.

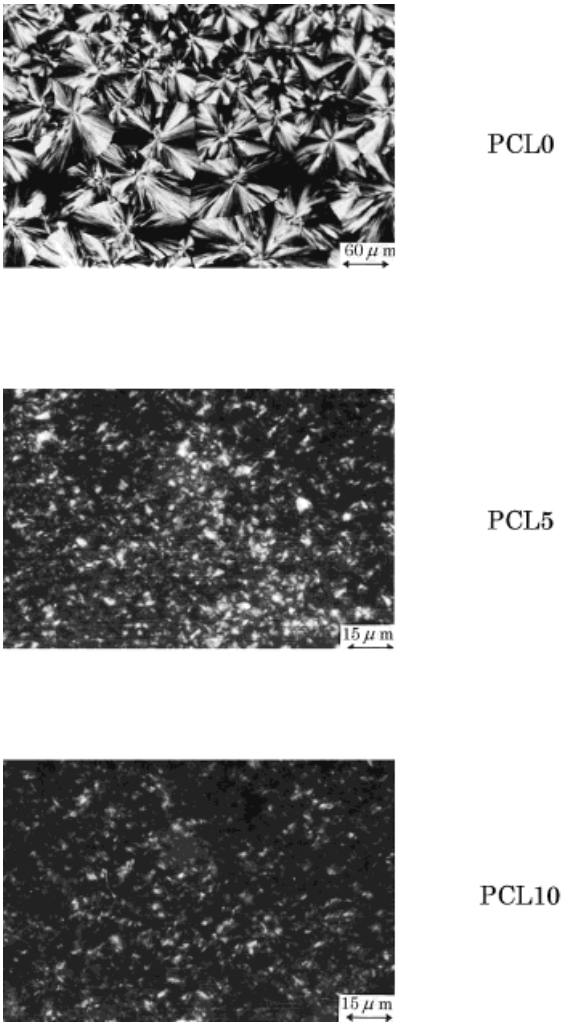

Figure 2 Microphotographs of PCL and two PCL–clay blends crystallized from the melt.

In the present work we synthesize a PCL–clay composite by using polymer intercalation from solution, and investigate its structural, thermal, and mechanical properties.

EXPERIMENTAL

Materials

Montmorillonite "Kunipia F" (MON) was supplied by Kunimine Ind. Co. This clay has exchangeable sodium ions, and a cation exchange

capacity of about 120 mequiv/100 g. PCL "PLACCEL-H7" was supplied by Daicel Chemicals, Ltd.

Preparation of Organophilic Clay

MON (1 g) and 50 mL of distilled water at 80°C were placed in a 100-mL beaker, and 1 g of distearyldimethylammonium chloride (DSAC) was added to the solution. The mixture was stirred vigorously for 1 h and then filtered, and the solid was washed three times with 100 mL of hot water to remove NaCl. The product was also washed with ethanol (50 mL) to remove any excess of ammonium salt, freeze-dried, and then kept in a vacuum oven at room temperature for 24 h. The resulting OMON dispersed well in chloroform, although the neat MON did not. Therefore, this organic modification was found effective.

Preparation of PCL–Clay Blends

A given amount of well-dried OMON and PCL pellets were placed in a Petri dish, hot chloroform was added, and the solution was kept at 50°C. After chloroform was vaporized, homogeneous films about 0.1 mm thick were obtained. The weight percentage of OMON in the blend is represented by Y in PCLY (e.g., PCL10 is a blend of PCL with 10 wt % of the organophilic clay). OMON will also be referred to as clay.

Characterization of the Blends

The blend films were drawn with a zone-drawing apparatus whose details are found in a previous article.[8] Morphologies of the PCL spherulites in the blends were observed on a polarizing optical microscope (Nikon Optiphot-Pol). The X-ray powder diffraction curves for the modified clay were recorded with a Mac Science PM-20 and CuKα radiation, and used to monitor the reaction between MON and DSAC. Wide-angle X-ray scattering (WAXS) photographs of the PCL–clay blends were taken with a flat camera having a pinhole slit, and using a Japan Electron Laboratory (JEOL, DX-GE-E) apparatus. Small-angle X-ray scattering (SAXS) photographs were also taken with a JEOL (JDX-8750) operated at 420 kV and 200 mA.

Thermal behavior of the blends was measured on a Seiko Instruments & Electronics DSC200 differential scanning calorimeter (DSC), at a heating rate of 10°C/min. T_m and heat of fusion (ΔH_m) were evaluated from a maximum position of the endothermic peak, and its area on the DSC curves, respectively.

Isothermal crystallization of the blends and neat PCL were carried out under a nitrogen atmosphere with a Perkin–Elmer DSC-7 apparatus. The neat PCL and the blends (5.3 ± 0.3 mg), encapsulated in aluminum pans, were heated to 100°C at a rate of 20°C/min, held 5 min at this temperature to destroy all crystallites, and cooled to an appropriate crystallization temperature (T_c = 40°C), at 200°C/min cooling rate.

Dynamic viscoelastic properties were measured with a Rheometrics Scientific RSA II Viscoelastic Analyzer. Temperature scans (from −130°C to 55°C) at 1 Hz frequency were carried out with a heating rate of 3°C/min.

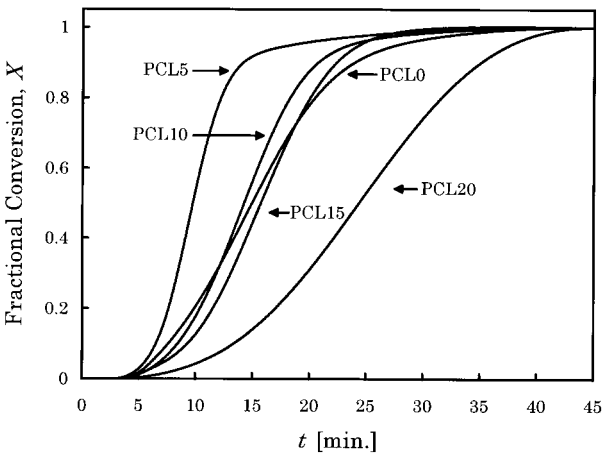

Figure 3 Isothermal crystallization for PCL and PCL–clay blends crystallized at 40°C.

Table I Effect of Clay Content on the Draw Ratio of PCL Blends

Sample	Draw Ratio
PCL0	3.3
PCL5	3.9
PCL10	4.7
PCL15	5.3
PCL20	5.6
PCL30	Brittle

Samples were drawn at 60°C.

RESULTS AND DISCUSSION

Thermal Behavior

The effect of the clay content on T_m and ΔH_m is shown in Figure 1. A straight line is drawn

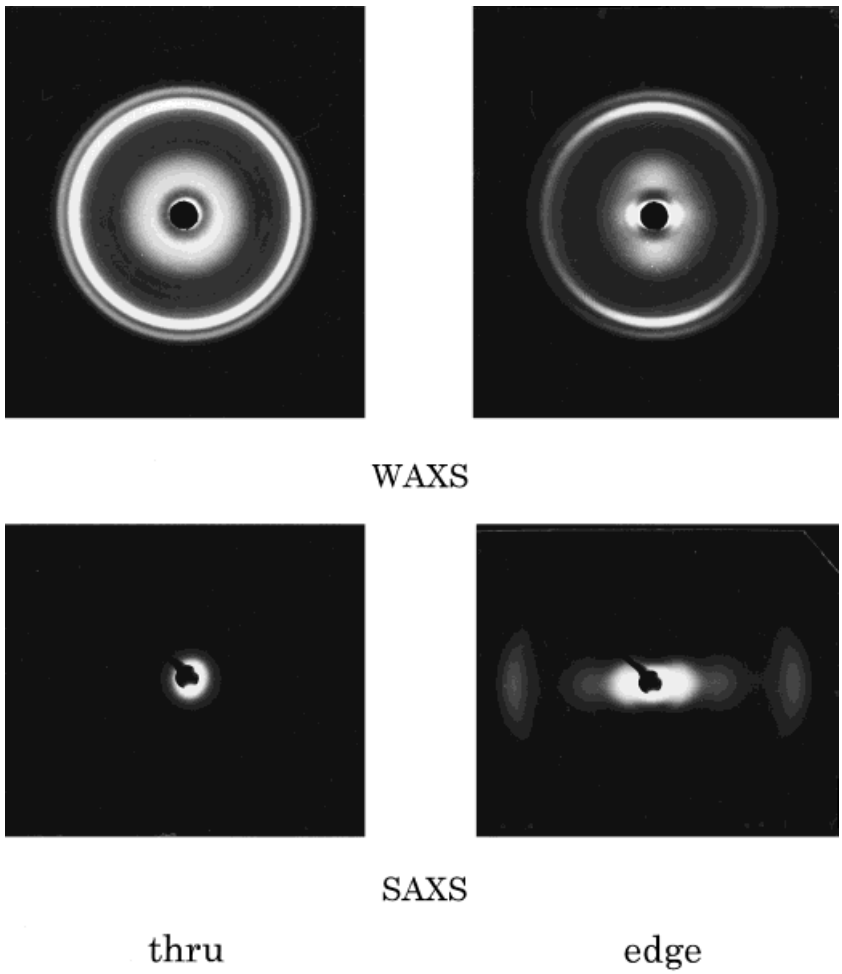

Figure 4 WAXS and SAXS photographs of undrawn PCL10.

through the values of ΔH_m at PCL0 and PCL100, where the value for ΔH_m at PCL100 equals zero. It can be seen that T_m decreases slightly with increasing clay content (ϕ_{mon}). It is also observed that the experimental ΔH_m values are almost on the straight line. This means that the crystallinity of PCL is practically independent of the amount of clay. Figure 2 shows PCL spherulites in PCL0, PCL5, and PCL10. It can be seen that the spherulite dimensions of PCL in the blends are smaller than those in the neat PCL. This result may imply that small PCL crystallites are formed in the presence of the clay. This conclusion is supported by the fact that T_m of PCL decreases with the addition of the clay (see Fig. 1).

From isothermal crystallization experiments, the fractional crystallinity conversion (X) was calculated as the ratio of the area under the exotherm at time t to the total area. Figure 3 shows the relationship between X and t. As can be seen, the X value of PCL5 is larger than that of PCL0 at a given t. However, when ϕ_{mon} is larger than 5%, X at a given t is noted to decrease with increasing ϕ_{mon}. Thus it can be said that a small amount of clay in the blend accelerates the crystallization of PCL, while a large clay content delays it. The overall isothermal crystallization rate is thought to be governed by two terms, namely, diffusion and nucleation.[11] The diffusion term is related to the activation free energy for transporting a polymer segment to a growing crystal face, and the nucleation term is related to the thermodynamic driving force for nucleation of new layers on the crystal. Considering these two terms, a small amount of clay seemed to serve as a nucleating agent, whereas a large amount of it seemed to hinder the transportation of polymer segments. Accordingly, we found that the clay has two opposing effects on the crystallization of PCL and, further, that these effects are dependent on the clay content.

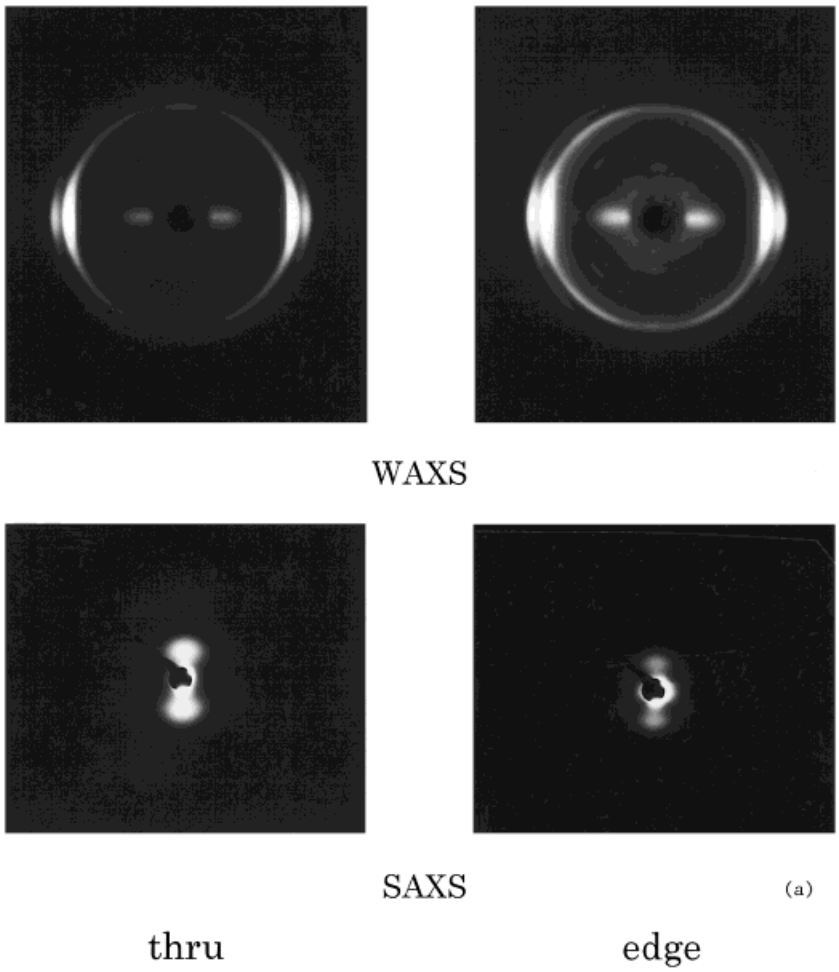

Figure 5 WAXS and SAXS patterns for drawn samples: (a) PCL0; (b) PCL5; (c) PCL10.

Table I shows the effect of ϕ_{mon} on the draw ratio for the neat PCL and its blends. The draw ratio increases with ϕ_{mon}. This means that the clay acts not as a stress concentrator but as a deformation accelerator at an elevated temperature. A reason for this is discussed below.

Structure of the PCL–Clay Blends

X-ray beam was incident on the as-cast film in the through and edge directions, and WAXS and SAXS photographs were taken; through and edge directions were perpendicular and parallel to the film surface, respectively. Figure 4 shows the photographs for the undrawn PCL10, where the equator for edge- and through-view patterns is aligned in the film-thickness direction. Figures 5(a–c) show the X-ray photographs for the drawn PCL0, PCL5, and PCL10, respectively. The drawn direction is parallel to the meridian in these diagrams. Figure 6 depicts the index assignment for some reflections seen in the edge-view patterns for PCL10 in Figures 4 and 5(c).

First, we shall discuss the photographs for the undrawn PCL10 (see Figs. 4 and 6). In the edge-view pattern of WAXS, strong and anisotropic intensity distribution can be seen around the beam stopper. Furthermore, a pair of intensity peaks which corresponds to the (001) reflection of OMON[12] can be seen on the equator near the beam stopper; the spacing for this plane is 1.8 nm, according to Bragg's law. However, the through-view pattern does not show these reflections. Moreover, we could neither see such strong intensity distribution nor detect the (001) reflection of OMON for both view patterns of the undrawn PCL0. These results suggest that the strong intensity distribution is derived from the

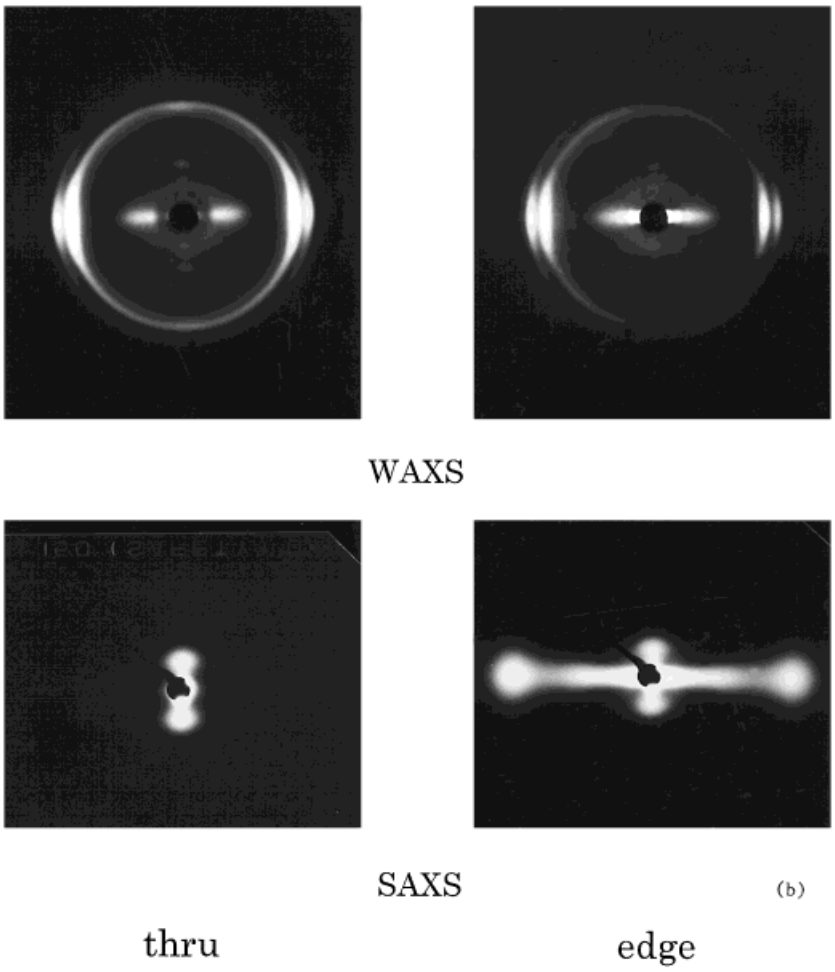

Figure 5 (*Continued from the previous page*)

presence of the clay, which possesses an anisotropic shape in the film. Since the intensity maxima that originate from the periodical clay layers (1.8 nm) can be seen clearly on the equator only for the edge-view pattern, the clay seems to exist in the film as a form of tactoids. These tactoids consist of some stacked clay layers with their surface planes lying almost parallel to the film surface. The edge-view WAXS pattern also shows arc-like reflections, corresponding to the (110) and (200) planes of PCL crystallites,[13,14] on the meridian, whereas the through-view pattern shows Debye–Scherrer rings, suggesting that the molecular axes are randomly oriented on the film plane. In addition, we found that the neat PCL0 did not exhibit such preferred orientation of PCL crystallites. These results mean that PCL molecules crystallize with their molecular chain axes (*c*-axis) perpendicularly oriented to the clay surface. The casting temperature used (50°C) is so high that preferred orientation may be developed under the influence of the clay. Since there existed an interaction between crystalline PCL and the clay, the PCL crystallites were probably formed on the clay surface. Concerning the SAXS photographs, only the edge-view photograph exhibits three pairs of intensity maxima on the equator; the intensity of the first peak (d_1 in Fig. 6) is very strong and appears near the beam stopper. The intensity distribution of the third peak (d_3 in Fig. 6) is broader than that of the second peak (d_2 in Fig. 6), and their spacings—calculated using Bragg's relation—are almost multiples of each other. Consequently, these two peaks can arise from the same periodic structural source. The long spacing calculated from these maxima was nearly 7.5 nm. Since the spacing of d_1 (about 19 nm) did not obey this multiple relationship, we assume that the first peak is derived from another structural unit, probably the crystalline lamella of

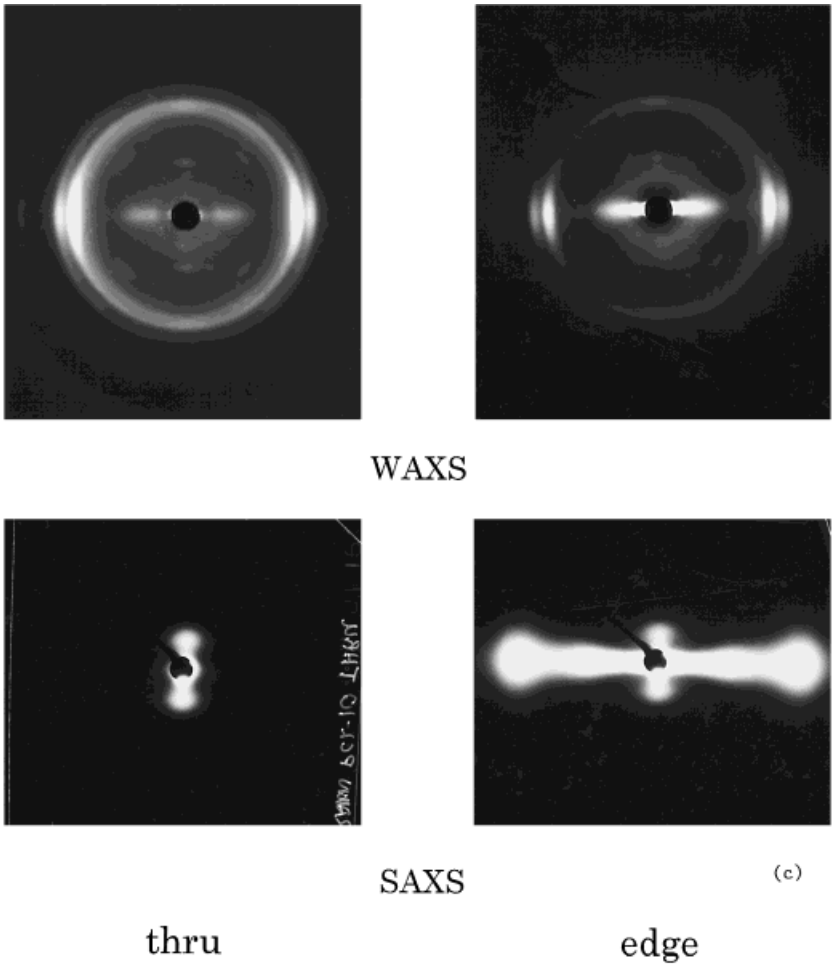

Figure 5 (*Continued from the previous page*)

PCL. It is shown below that the second and third peaks are not derived from the lamellar structure of PCL crystallites. Instead, these peaks are considered to be caused by the existence of the tactoids. The appearance of these reflections implies that these tactoids form the superlattice with a long period in the thickness direction of the film. The surface of the tactoids is supposed to be almost parallel to the film surface, while crystalline PCL lamellae are probably inserted between the parallel tactoids. The spacing between lamellae (19 nm) is larger than that between tactoids (7.5 nm), as described above. Thus it seems that the lamellae are sparsely formed onto the parallel tactoids, and that such location of the lamellae may result in a longer period between them. By taking account of the long period of tactoids (7.5 nm) and the spacing of the clay layers (1.8 nm), the number of the silicate monolayers forming the tactoids was calculated and found to be less than 4. It is likely, then, that delamination of the clay layers does not take place in the PCL–OMON blends during the solvent-casting process used in this work; such a result has been also obtained in the PLLA–clay blends.[8] However, this orientation of the tactoids is assumed to impart an excellent water-barrier property to the blends, as reported for NCH.[15]

Now let us consider the photographs for the drawn samples (see Figs. 5 and 6). The edge- and through-view patterns of SAXS exhibit long periodic reflections on the meridian parallel to the drawing direction in spite of ϕ_{mon}. Apparently, these reflections are derived from the stack of the PCL crystalline lamellae formed during the drawing process. We noted that the SAXS photographs of the blends [Figs. 5(b,c)] show a streak on the equator only in the edge-view patterns, whereas the neat PCL0 [Fig. 5(a)] does not show it. Furthermore, because this streak is not seen for the

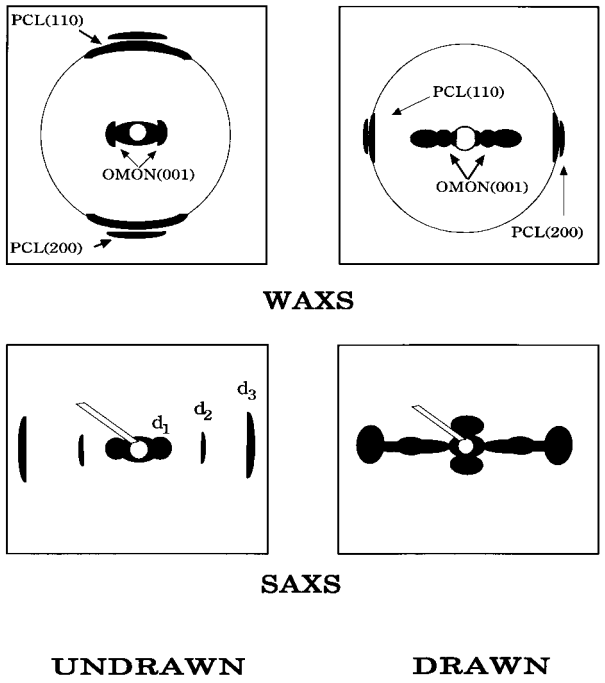

Figure 6 Index assignment of some reflections observed for PCL10 in Figures 4 and 5(c).

undrawn PCL10 (see Fig. 4), the streak can be considered to be caused not by the existence of the clay but by the planelike voids or fibrils; these voids or fibrils are probably developed during the drawing process of the blends, on the plane parallel to the tactoid surface. Two pairs of intensity maxima can also be observed on the streak in Figures 5(b,c). Judging from their peak positions, they can be considered to correspond to those seen in the undrawn PCL10 blend (see Figs. 4 and 6). However, the intensity distribution in the azimuthal direction of these maxima is relatively narrow in comparison with that obtained for the undrawn sample. Therefore, the orientation of the tactoids seems to be increased by drawing. We evaluated a long spacing from the second and third reflections (middle- and highest-angle values, respectively) of the SAXS patterns in Figure 5(c). It was around 7.2 nm, which is somewhat smaller than that obtained for the undrawn PCL10 (7.5 nm).

WAXS patterns of the drawn PCL blends show a difference in the intensity distribution near the beam stopper between edge- and through-views; that is, a pair of oriented intensity maxima, originating from the (001) plane of the clay, can be seen on the equator only for the edge-view pattern. This reflection can be noted by a careful comparison between the corresponding WAXS patterns for the PCL0, PCL5, and PCL10 samples shown in Figures 4 and 5. Clearly, it means that delamination of the clay layers does not take place, even under a shear force applied during the hot drawing process.

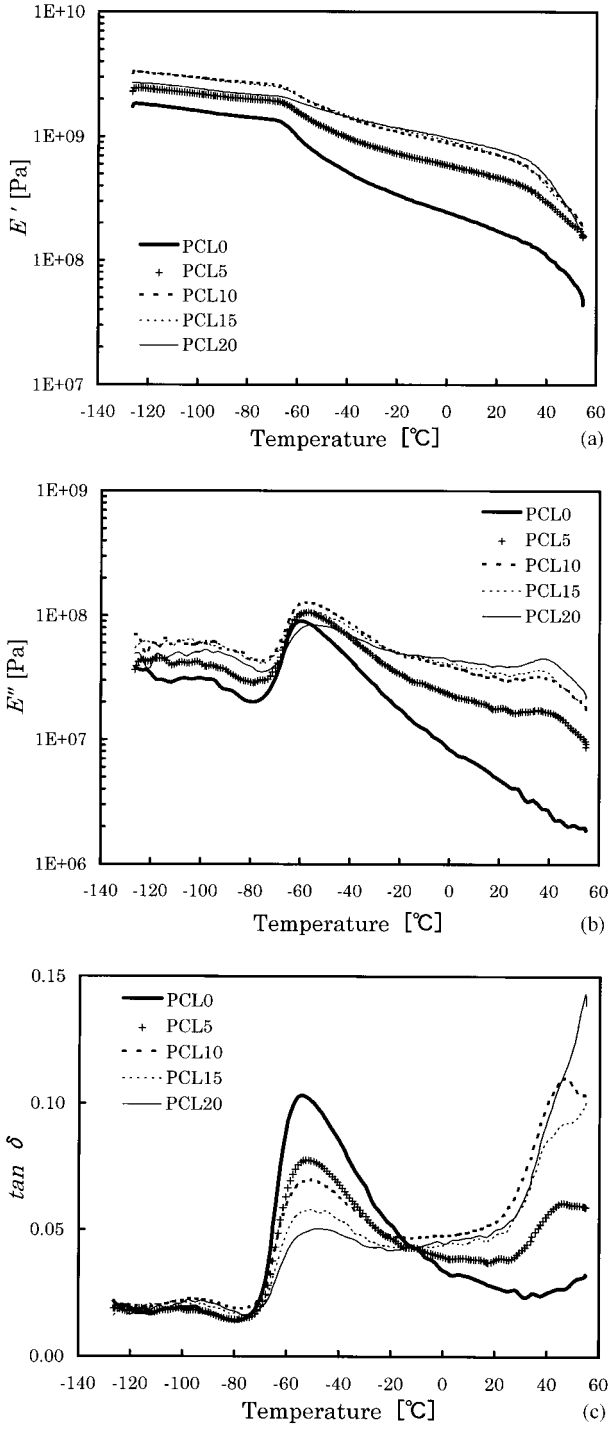

Figure 7 Dynamic viscoelastic behavior of PCL–clay blends: (a) E'; (b) E''; (c) tan δ.

Table II Effect of Clay Content on Thermal Transition Temperatures of PCL

Sample	T_g (°C)	T_{CH_2} (°C)	T_{int} (°C)
PCL0	−54.1	−101.7	—
PCL5	−52.2	−101.4	36.9
PCL10	−51.1	−95.8	36.6
PCL15	−50.3	−101.4	35.2
PCL20	−47.5	−97.6	37.7

T_g, glass transition temperature measured from tan δ curve; T_{CH_2}, relaxation of methylene chains measured from tan δ curve; T_{int}, collapse of interaction between PCL crystallites and clay measured from E'' curve.

Although we cannot discuss further the relationship between macroscopic and microscopic drawing mechanisms of the PCL–clay blends, we can conclude that fibrillation occurs during the drawing process of the blends, accompanying the formation of planelike voids that are parallel to the film surface. As previously stated, the draw ratio of PCL is increased by the addition of the clay. This result is probably related to the fibrillation mechanism explained above; that is, fibrillation can easily take place between the tactoids in the blends. Consequently, a high draw ratio can be attained in the PCL–clay blends.

Dynamic Mechanical Properties

Figure 7(a–c) shows the temperature dependence of the storage E', loss E'' tensile modulus, and tan δ of the blends, respectively. In spite of the clay content, E' decreases with increasing temperature and a transition can be seen at about −60°C. Roughly speaking, E' at a given temperature increases with increasing ϕ_{mon}. Furthermore, the temperature dependence of E' of the samples containing the clay is weaker than that of PCL0. Thus it seems that E' is retained at a high level over a wide temperature range by the addition of the clay. This can be due to the clay restricting the molecular motions of PCL. The tan δ curves show a large maximum at $T = -54$°C, which corresponds to T_g of PCL; this value is similar to that reported for a crystalline annealed PCL.[16] In these plots, a low-temperature transition, which corresponds to the relaxation of local motions of methylene units in the main chain, can be observed at about $T = -100$°C for all the samples[17]; this transition temperature is referred as T_{CH_2}. The values of T_g and T_{CH_2} are presented in Table II. Although T_{CH_2} is independent of ϕ_{mon}, T_g increases slightly with increasing ϕ_{mon}. Since the increase is not so large, the interaction between the clay and amorphous PCL molecules seems to be not so strong. In other words, intercalation does not seem to take place in the PCL–OMON blends. If intercalation occurred, T_g for the matrix polymer would be absent because the polymer chains were confined to the two-dimensional galleries of the layered clay material, even by the addition of a small amount of the clay.[18] The value for tan δ at T_g decreases with increasing ϕ_{mon}. This means that the dispersion energy at T_g decreases as the clay content increases. Such phenomenon has been also observed in PLLA–clay blends.[8] Moreover, tan δ values for the samples containing the clay increase when temperature is near the PCL melting point. At this high temperature range, we can see a maximum at T_{int} in the E'' plots only for the PCL–clay blends, [see Fig. 7(b) and Table II]. Therefore its appearance is considered to be caused by the molecular relaxation inside the PCL crystallites formed under the influence of the clay. In other words, this transition probably reflects the collapse of the interaction between PCL crystallites and the clay. The existence of such interaction has been pointed out in previous sections, and it probably retains a high value of E' up to near the melting point of the PCL matrix.

Accordingly, it was found that intercalation of PCL in OMON does not take place largely in the PCL–clay blends prepared using the solvent-cast method attempted in this work, nor does delamination occur during the drawing process. However, it should be noted that the organophilic clay in the blends showed a structure of characteristic geometry. An interaction between the clay and PCL was developed and, consequently, preferred orientation of the PCL crystallites was induced.

REFERENCES

1. A. Akelah and A. Moet, *J. Appl. Polym. Sci.: Appl. Polym. Symp.,* **55,** 153 (1994).
2. A. Usuki, Y. Kojima, M. Kawasumi, A. Okada, Y. Fukushima, T. Kurauchi, and O. Kamigaito, *J. Mater. Res.,* **8,** 1179 (1993).
3. Y. Kojima, A. Usuki, M. Kawasumi, A. Okada, Y. Fukushima, T. Kurauchi, and O. Kamigaito, *J. Mater. Res.,* **8,** 1185 (1993).
4. Y. Kojima, A. Usuki, M. Kawasumi, A. Okada, T. Kurauchi, and O. Kamigaito, *J. Appl. Polym. Sci.,* **49,** 1259 (1993).

5. K. Yano, A. Usuki, A. Okada, T. Kurauchi, and O. Kamigaito, *J. Polym. Sci., Part A: Polym. Chem. Ed.,* **31,** 2493 (1993).
6. P. B. Messersmith and E. P. Giannelis, *Chem. Mater.,* **6,** 1719 (1994).
7. P. B. Messersmith and E. P. Giannelis, *Chem. Mater.,* **5,** 1064 (1993).
8. N. Ogata, G. Jiménez, H. Kawai, and T. Ogihara, *J. Polym. Sci., Part B: Polym. Phys. Ed.,* to appear.
9. J. Heuschen, R. Jérôme, and P. Teyssié, *J. Polym. Sci.: Polym. Phys. Ed.,* **27,** 523 (1989).
10. P. B. Messersmith and E. P. Giannelis, *J. Polym. Sci., Part A: Polym. Chem. Ed.,* **33,** 1047 (1995).
11. J. G. Fatou, *Makromol. Chem., Suppl.,* **7,** 131 (1984).
12. Y. Fukushima, *Clays and Clay Minerals,* **32,** 320 (1984).
13. H. Bittiger and R. H. Marchessault, *Acta Cryst.,* **B26,** 1923 (1970).
14. Y. Chatani, Y. Okita, H. Tadakoro, and Y. Yamashita, *Polym. J.,* **1,** 555 (1970).
15. N. Ogata, T. Ogawa, T. Ida, T. Yanagawa, T. Ogihara, and A. Yamashita, *Sen-i Gakkaishi,* **51,** 439 (1995).
16. J. V. Koleske and R. D. Lundberg, *J. Polym. Sci., Part A-2,* **7,** 795 (1969).
17. A. V. Tobolsky, in *Polymer Science and Materials,* A. V. Tobolsky and H. F. Mark, eds., Wiley, New York, 1971, Chap. 10.
18. R. A. Vaia, H. Ishii, and E. P. Giannelis, *Chem. Mater.,* **5,** 1694 (1993).